

THIS DOCUMENT AND EACH AND EVERY  
PAGE HEREIN IS HEREBY RECLASSIFIED

FROM Conf TO Unclass  
AS PER LETTER DATED NACA Release  
notice #122

CHANCE VUGHT CORPORATION LIBRARY

NATIONAL ADVISORY COMMITTEE FOR AERONAUTICS

SPECIAL REPORT #70.

THE TRANSITION PHASE IN THE TAKE-OFF OF AN AIRPLANE

By J. W. Wetmore  
Langley Memorial Aeronautical Laboratory

S. R. 70  
SPECIAL RPT

December 1937

# THE TRANSITION PHASE IN THE TAKE-OFF OF AN AIRPLANE

By J. W. Wetmore

## SUMMARY

An investigation was undertaken to determine the character and importance of the transition phase between the ground run and steady climb in the take-off of an airplane and the effects of various factors on this phase and on the air-borne part of the take-off as a whole. The information was obtained from a series of step-by-step integrations, which defined the motion of the airplane during the transition and which were based on data derived from actual take-off tests of a Verville AT airplane. Both normal and zoom take-offs under several loading and take-off speed conditions were considered. The effects of a moderate wind with a corresponding wind gradient and the effect of proximity of the ground were also investigated.

The results show that, for normal take-offs, the best transition was realized at the lowest possible take-off speed. Moreover, this speed gave the shortest over-all take-off distance for normal take-offs. Zoom take-offs required a shorter over-all take-off run than normal take-offs, particularly with a heavy loading, if the obstacle to be cleared was sufficiently high, e.g., greater than 50 feet; no advantage was indicated for the airplane with a light loading if the height to be cleared was less. The error that would result from the neglect of the transition in the calculation of the air-borne distance of take-off was found to vary from 4 percent with the heaviest loading considered to -4 percent with the lightest loading for normal take-offs over a 100-foot obstacle; the percentage error was twice as great for a 50-foot obstacle. For zoom take-offs the error attained much greater values. The average wind gradient corresponding to a 5-mile-per-hour surface wind reduced the air-borne distance required to clear a 50-foot obstacle by about 9 percent with the lightest loading and 16 percent with the heaviest loading; for a 100-foot obstacle the reduction was about 10 percent in both cases. The over-all reduction due to this wind was approximately twice that resulting from the wind gradient alone. A simple expression for the reduction of observed take-off performance to no-wind conditions is presented. Ground effect is shown to reduce the air-borne distance to attain a height of 50 feet by 10 percent with the lightest loading and 16 percent with the heaviest loading; for a 100-foot obstacle the percentage reduction was about one-half as great.

## INTRODUCTION

In the process of taking off, the course of an airplane consists of three phases: a run along the ground to attain flying speed, a transition curve in which the flight path changes from the horizontal direction of the ground run to an inclination suitable for climbing, and a more or less steady climb to a height at which any obstacles at the edge of the airport will be surmounted. The motion of an airplane in the ground-run and steady-climb stages is relatively simple and therefore can be predicted for prescribed conditions with reasonable accuracy, presupposing an adequate knowledge of the airplane characteristics. The transition, on the other hand, can be accurately defined only by very complex relations; hence, common practice in calculating take-off performance has been to regard this phase as negligible or to account for it with approximations of uncertain validity.

The investigation described herein was undertaken to provide an indication of the character and relative importance of the transition and of the effects of various factors on the transition itself and on the air-borne portion of the take-off as a whole. For this purpose a series of take-off tests was conducted with a conventional biplane. The tests included both normal take-offs, wherein the air speed was maintained as nearly constant as possible from the instant of leaving the ground, and zoom take-offs, in which the speed was reduced after leaving the ground. The test conditions for each type of take-off covered two loadings and several take-off speeds. The motion of the airplane in the take-offs was measured with a recording photodolite.

The results of these tests were not used directly, as originally intended, inasmuch as they were found to be confused by rather wide variations in piloting procedure and wind condition. Instead, the force relations pertaining to the airplane under take-off conditions were derived from data provided by the tests and served as the basis for a series of step-by-step integrations whereby the motion of the airplane during take-off was determined for various conditions without the effects of piloting and wind. The calculations covered the range of loading and speed conditions included by the actual tests, and an additional loading condition was also considered.

A measure of the effect of ground proximity on the airplane characteristics was obtained from the test data and, with this information, the influence of ground effect on the take-off was investigated for each of two loading conditions. For the same conditions the effects of a wind increasing in velocity with altitude were also evaluated.

#### APPARATUS

A Verville AT airplane (fig. 1) was used for the take-off tests. The pertinent characteristics of this airplane are given in table I. The following standard N.A.C.A. recording instruments were mounted in the airplane: an air-speed recorder; an accelerometer located near the center of gravity and recording accelerations along the normal, or Z, axis of the airplane; an inclinometer recording the direction of the resultant of the external forces imposed on the airplane; a recording engine tachometer; and a control-position recorder connected to the elevators. Half-second intervals of time were recorded by all the instruments from impulses produced by a standard timer.

An N.A.C.A. recording phototheodolite, essentially a combination of a motion-picture camera and a recording theodolite, provided records from which the horizontal and vertical displacements of the airplane relative to the ground and its attitude angle could be determined at intervals of 1/16 second. A timer was also used in conjunction with this instrument.

Synchronization of the phototheodolite records with those of the airplane instruments was accomplished by means of an electrically operated device mounted on the landing gear of the airplane and connected through the instrument switch so that, at the instant the pilot threw the switch to start the instruments, a quantity of white powder was discharged and formed a cloud that was readily discernible in the photographs.

The wind speed at the ground was measured with an indicating vane anemometer.

#### TEST PROCEDURE

A series of eight take-offs was made with each of two

loading conditions: 2,060 pounds and 2,378 pounds gross weight. For four of the take-offs of each series, which will be designated "normal" take-offs, the pilot was requested to leave the ground at speeds ranging from 3 to 15 miles per hour in excess of the minimum level-flight speed and to climb at the same speeds, attaining steady climbing conditions as quickly as possible. For the four remaining runs, given the designation of "zoom" take-offs, the speeds at the instant of take-off were in the same range but were reduced after the airplane left the ground, the climbs in all cases being made at a speed slightly in excess of the minimum. In all the take-offs the airplane was headed directly into the wind. The engine was operated at full throttle throughout each run.

The phototheodolite was set up on the ground at a suitable distance from the course of the airplane and recorded its motion during the latter third of the ground run and throughout the transition and climb to a height of about 100 feet. The procedure followed in the operation of the phototheodolite and in the evaluation of the data obtained therefrom was substantially the same as that described for the landing tests of reference 1, although the instrument used for the present tests is of a later and improved design.

#### COMPUTATIONS

The results of the foregoing tests gave evidence of sufficiently great irregularities in the wind conditions and piloting to obscure completely the effects that the tests were expected to disclose; hence, the purpose of the investigation was not directly accomplished by the tests alone. The data obtained from the take-off tests, however, made possible the derivation of the force relations required as the basis for a series of step-by-step integrations defining the motion of the airplane during take-off for various conditions. In this way the troublesome factors of wind and piloting were eliminated.

Derivation of force relations.— Synchronized readings of the data recorded by the airplane instruments and the phototheodolite during the take-offs were made at frequent intervals throughout the records, thus covering a considerable range of flight conditions. Values of lift and excess thrust were obtained for each set of readings according to the following procedure. The normal and longitudinal

components of the aerodynamic forces acting on the airplane  $F_z$  and  $F_x$ , respectively, were determined from the relations

$$F_z = \frac{W}{g} a_z$$

and

$$F_x = \frac{W}{g} a_z \tan \theta$$

where  $W$  is the gross weight of the airplane

$g$ , the acceleration of gravity

$a_z$ , the normal acceleration as recorded by the accelerometer

$\theta$ , the angle of the inclinometer pendulum relative to the normal axis of the airplane

The flight-path angle  $\gamma$ , referred to wind axes, was given by

$$\gamma = \sin^{-1} \frac{V_v}{V}$$

where  $V_v$  is the vertical velocity, determined by differentiation of the time-distance curves derived from the phototheodolite records

$V$ , the air speed along the flight path

It was necessary, of course, to assume here that the wind had no vertical component, apparently a reasonable assumption for average conditions according to the information of reference 1.

The angle of attack  $\alpha$  was then obtained from

$$\alpha = \lambda - \gamma$$

where  $\lambda$  is the attitude angle of the airplane, provided by the phototheodolite records. With the foregoing information, it was possible to determine values for the lift  $L$  and the excess thrust  $T_{ox}$  by resolving the forces  $F_x$  and  $F_z$  along the flight-path axes or

$$L = F_Z \cos \alpha + F_X \sin \alpha = \frac{W}{g} a_z (\cos \alpha + \tan \theta \sin \alpha)$$

$$T_{ex} = F_X \cos \alpha - F_Z \sin \alpha = \frac{W}{g} a_z (\tan \theta \cos \alpha - \sin \alpha)$$

The values of lift were converted to the coefficient form  $C_L$  with the relation  $C_L = \frac{L}{\frac{1}{2} \rho S V^2}$ . Thus the data could readily be plotted and faired as a function of angle of attack. (See fig. 2.)

The full-throttle excess thrust is, in effect, a function of two variables, angle of attack and air speed. It would consequently be difficult to plot these data directly. For this reason the effective propeller thrust  $T$ , shown in figure 3, was calculated by means of the information provided in references 2 and 3. The drag  $D$  could then be determined from the equation  $D = T - T_{cx}$  and

thence the drag coefficient  $C_D = \frac{D}{\frac{1}{2} \rho S V^2}$  which could, of

course, also be plotted as a function of angle of attack to establish a suitably faired curve. With the data in this form, the relation of excess thrust to air speed and lift coefficient was determined by using the faired results in a reversal of the procedure.

In order to take into account the effect of ground proximity on the lift and drag characteristics, hence on the excess thrust, the data were divided into two groups and were plotted separately, according to whether they were obtained when the wheels of the airplane were above or below a height of 10 feet from the ground. This height was arbitrarily chosen as the line of demarcation between the region of strongest ground effect and the region in which, for the purposes of the present investigation, the ground effect could be considered as negligible. The data available were insufficient to warrant further division.

The lift and drag coefficients evaluated by the foregoing methods are plotted against angle of attack in figure 2. In figure 3 the excess thrust within and outside of the region of principal ground effect is shown as a function of lift coefficient and air speed.

Step-by-step integrations.— At quarter-second intervals throughout the transition phase of the take-off, the vertical acceleration  $a_v$  and the horizontal acceleration  $a_h$  of the airplane were calculated by successive approximations according to the relations

$$a_v = \frac{g(L \cos \gamma + T_{ex} \sin \gamma - W)}{W}$$

and

$$a_h = \frac{g(T_{ex} \cos \gamma - L \sin \gamma)}{W}$$

Corresponding velocities were determined from

$$V_v = V_{v_0} + \frac{0.25(a_{v_0} + a_{v_1})}{2} + \frac{0.25(a_{v_1} + a_{v_2})}{2} + \frac{0.25(a_{v_{n-1}} + a_{v_n})}{2}$$

and

$$V_h = V_{h_0} + \frac{0.25(a_{h_0} + a_{h_1})}{2} + \frac{0.25(a_{h_1} + a_{h_2})}{2} + \frac{0.25(a_{h_{n-1}} + a_{h_n})}{2}$$

Vertical and horizontal displacements were similarly determined; the flight-path angle was obtained from

$$\gamma = \tan^{-1} \frac{V_v}{V_h}$$

The initial values of  $a_v$  and  $V_v$ , i.e., at the instant of leaving the ground, were, of course

$$a_{v_0} = 0$$

and

$$V_{v_0} = 0$$

The horizontal speed  $V_{h_0}$  at the same instant was the assumed take-off speed and, since at this instant

$$L = W$$



the value of the excess thrust  $T_{ex}$  and thence the value of  $a_{h_0}$  could be determined. For subsequent intervals the quantities involved in the calculations were determined by the usual methods of successive approximation.

The course of the lift coefficient in the early part of the transition was prescribed by the assumption that the transition should be of as short duration as possible. This limitation, of course, required that the airplane be pulled up quickly to the angle of attack for maximum lift coefficient, as soon as the desired speed for taking off was attained, and held at this angle as long as possible. The lift coefficient was then reduced in time to prevent the flight-path velocity from decreasing, by reason of the increasing climb angle, below the value designated for the steady climb and to permit the adjustment of the lift coefficient necessary to provide a smooth approach to the steady-climb conditions without exceeding reasonable values for the corresponding rate of change of the angle of attack. Examples of the variation in lift coefficient followed in performing the calculations are shown in figure 4.

The excess thrust corresponding to the lift coefficient and speed occurring at a particular instant was taken from the curves of figure 3, according to whether the height at that instant was greater or less than 10 feet. In this way allowance was made for the ground effect.

The computations covered three loading conditions: gross weights of 2,060 pounds, 2,378 pounds, and 2,800 pounds. For each load the calculations were carried through for three normal take-offs at different speeds ranging from an assumed minimum allowable speed to 20 percent in excess of this value. Similarly, two zoom take-offs were calculated for take-off speeds 10 percent and 20 percent greater than the minimum allowable speed at which the final steady climb was assumed to be made in both cases. The minimum allowable speed was arbitrarily taken as 4 percent in excess of the speed corresponding to the maximum lift coefficient, 1.3. For all the foregoing conditions there was assumed to be no wind.

The effects of wind were determined for two cases: one with the heaviest loading and the other with the lightest loading. For these cases there was introduced into the calculations a wind velocity of 5-miles-per-hour mag-

nitude at the ground, increasing with height according to the relationship given by reference 1 as representing an average wind gradient, which is

$$\frac{V_w}{V_{w_0}} = \left( \frac{H_e}{H_0} \right)^{1/7}$$

where  $V_{w_0}$ , which was assigned a value of 5 miles per hour, is the wind speed corresponding to  $H_0$ , the effective height of the airplane while in contact with the ground, assumed to be 5 feet; and  $V_w$  is the wind speed at any other effective height  $H_e$ , i.e., the height of the wheels above the ground plus 5 feet.

For the same two loading conditions, the effect of ground proximity on the air-borne phase of take-off was investigated by using the excess-thrust data obtained above the 10-foot level, hence sensibly outside the influence of ground effect, throughout the integrations and comparing the results with those obtained for similar cases in which the ground effect was included.

The ground-run phase of the take-off was considered only insofar as was necessary to show the effects of variations in take-off speeds and methods on the complete take-off. In all cases only the distance required to accelerate from a common speed of 75 feet per second up to the take-off speed was calculated. In the determination of these distances, the rolling-friction coefficient was assumed to be 0.05, corresponding to an average turf surface. The air forces were taken from the data obtained within the region of ground effect.

## RESULTS

A summary of the results obtained from the calculations is given in table II. Figures 5 through 7 show the calculated flight paths of the airplane during the transition and steady climb for all the conditions investigated. In figure 8 the distance on the ground required to accelerate from a speed of 75 feet per second to the take-off speed is plotted against take-off speed for the three loading conditions. Figures 9 through 11 show the variation due to take-off speed in the air-borne distances required

to clear heights of 50 and 100 feet for both normal and zoom take-offs. These figures also show the effect of take-off speed on the over-all take-off distance, i.e., including the ground run after a velocity of 75 feet per second is attained.

Figure 12 shows the percentage difference for various take-off speeds between the air-borne distance as calculated by the methods previously described, where due consideration was given to the transition, and the distance that would be obtained were the transition to be neglected. For the normal take-offs, the latter value for the distance was taken as

$$D = \frac{H}{\tan \gamma}$$

where  $H$  is the obstacle height to be cleared and  $\gamma$  is the flight-path angle corresponding to a given speed. This relation was based on the assumption that steady-climbing conditions obtained from the instant of leaving the ground. For the zoom take-offs the most obvious approximate relation for the air-borne distance appeared to be

$$D = \frac{H - \frac{V_1^2 - V_2^2}{2g}}{\tan \gamma}$$

where  $V_1$  and  $V_2$  are the initial and final flight-path velocities, respectively; and  $\gamma$  is the flight-path angle corresponding to  $V_2$ . This equation was based on the assumptions that constant excess power was available throughout the climb and that steady conditions were realized before the height  $H$  was attained. Figure 12 is intended to indicate the extent to which the take-off is affected by the transition and the magnitude of the error that might be introduced by the neglect of the transition in the calculation of take-off distances.

The effect on the air-borne distance of an average wind gradient corresponding to a surface wind velocity of 5 miles per hour is shown in figure 13 for normal take-offs with the heaviest and lightest loads. In figure 14 the influence of ground effect is shown for the same loading conditions.

## DISCUSSION

The nature of the flight path during the transition phase of the take-off is shown in figures 5, 6 and 7. The initially increasing slope of the path followed later by a decrease is apparently characteristic, at least for the airplane and conditions considered herein. In the case of normal take-off, the reason for this reversal of curvature lies in the fact that the airplane continues to accelerate immediately after leaving the ground and, in being slowed to its original speed, assumes a climbing angle too steep to be maintained. The flight-path angle must therefore be reduced to a value at which the airplane can climb steadily. The flight paths for the zoom take-offs have a generally similar shape, but variations in the slope are more pronounced owing to the greater changes in speed.

Inasmuch as most airplanes probably have, in part by virtue of the ground effect, an excess of thrust in the initial stage of the transition and hence will accelerate, it is likely that the form of the transition curve shown is representative of the form that would generally be experienced.

The procedure that would be required in controlling an airplane along a path such as that described is indicated in figure 4. The control column would first be pulled back to put the airplane in an attitude of high lift and held until the angle of climb was sufficient to cause a deceleration. It would then be pushed forward to reduce the angle of attack to a value considerably below that corresponding to the steady climb in time to prevent the speed from dropping below that prescribed for the climb. Finally, it would again be pulled back as the angle of climb decreased so that the correct flight-path angle and angle of attack for steady climbing might be simultaneously realized. In practice, it would probably not be possible to synchronize, exactly, the attainment of the proper flight-path angle and angle of attack; consequently, an oscillatory rather than a steady flight path would result. If sufficient effort were made to maintain constant speed, however, the amplitude of the oscillation would not be great and the mean flight path would probably correspond closely to the one that would be obtained under steady conditions.

For normal take-offs, it is apparent from the curves

of figures 5, 6, and 7 that, insofar as the transition alone is concerned, the optimum take-off speed, in the range considered, is the lowest value shown. Higher speeds provide an initially greater excess of lift and, consequently, a higher vertical acceleration, so that the transition is completed more quickly and with less variation in forward velocity. At the slower speed, however, there is a greater excess thrust available which, although partly converted to kinetic energy at first, eventually goes toward increasing the height or potential energy of the airplane; thus, when the transition is completed, the height attained is greater in proportion to the horizontal distance covered than that for the higher-speed take-offs.

The maximum angle of climb occurs at approximately the intermediate speed shown so that, in the range of speeds between the minimum and that for best angle of climb, the effects of variations in take-off speed on the transition and on the steady climb are opposed. For an obstacle height of 50 feet a considerable portion of the air-borne distance is occupied by the transition so that the opposing effects are nearly balanced. Hence there is little change in the air-borne distance with increasing take-off speed up to the speed for best angle of climb (figs. 9, 10, and 11); beyond this speed the distance, of course, increases. Obviously then since the ground-run distance (fig. 8) increases with the take-off speed, the shortest over-all take-off distance required to gain a height of 50 feet, in a normal take-off, would be realized with the lowest possible take-off speed.

With an obstacle height of 100 feet the transition is a relatively small part of the air-borne distance. The effect of take-off speed on the steady climb is therefore predominant and consequently the shortest air-borne distance occurs at or near the speed for best angle of climb. The reduction in air-borne distance, however, is more than offset by the increased ground run so that, in this case also, the lowest take-off speed gives the shortest over-all distance.

In zoom take-offs the airplane is held in contact with the ground until the speed reaches a value considerably above the minimum flying speed. It is then pulled off abruptly into a steep climb during which the speed is reduced. It may be shown that an airplane running along the ground at its most efficient attitude, i.e., the atti-

tude corresponding to the minimum value of  $C_D - \mu C_L$ , will ordinarily have, in the range of speeds between the minimum flying speed and a speed considerably in excess of the minimum, appreciably less resistance, hence greater excess thrust, than if it were completely air-borne at similar speeds. The excess kinetic energy gained in running a given distance along the ground would be greater, therefore, than the potential energy that might be gained in flight in the same distance. Thus, if the excess kinetic energy could be converted to potential energy without too great loss, it should be possible to attain a greater height in a given distance from a zoom take-off than from the shortest normal take-off. This argument is borne out in figures 9, 10, and 11 for an obstacle height of 100 feet where, with the lightest load, the total horizontal distance required to gain this height from a ground speed of 75 feet per second is about 5 percent less for the shortest zoom take-off than for the shortest normal take-off; with the heaviest load there is a larger difference, about 17 percent, owing to the fact that, with other conditions remaining equal, the difference between the excess thrust on the ground and that in flight increases with increasing weight.

In figures 5, 6, and 7 it will be noted that in some cases, particularly with the lighter loads and higher take-off speeds, the height attained before the conversion of energy is completed is greater than 50 feet. In these cases, at an obstacle height of 50 feet, there is still an excess of kinetic energy remaining, which is equivalent to a loss. Therefore the zoom take-off provides little or no advantage over the normal take-off, as may be seen in figures 9, 10, and 11.

An indication of the extent of the error that might be introduced into the calculation of take-off performance by the neglect of the transition is provided in figure 12. This figure shows the percentage difference between the air-borne distance as calculated by the rigorous method and the distance resulting from the assumption that the change from the conditions of the ground run to those of the steady climb occurs instantaneously and without effective loss of energy. For normal take-offs over a 100-foot obstacle the error ranges from a maximum positive value of about 4 percent with the heaviest load, i.e., the approximate distance is too great, to a maximum negative value of the same magnitude. The fact of a positive error

is undoubtedly attributable to the influence of ground effect. With a 50-foot obstacle height the error is about twice as great in the same sense for corresponding conditions, since the error in actual distance is about the same.

For the zoom take-offs over a 100-foot obstacle, the error is comparable at the lower take-off speeds with that for the normal take-offs but becomes increasingly negative as the take-off speed departs more from the minimum value. The largest error in this case, in the range of conditions covered, occurs with the lightest load and has a negative value of about 10 percent. For the 50-foot obstacle height, the error increases rapidly with take-off speed to very large values, particularly with the lighter loads. The large errors are due to the fact that the conversion from kinetic to potential energy is not completed until after the 50-foot height has been reached, in which case the assumption of an instantaneous change from ground-run to steady-climb conditions is not justified.

The scope of this investigation is not sufficiently wide for a definite determination of the relationship that might exist between this error and the airplane characteristics, but it is believed that this relationship could be established with the aid of similar data for other types of airplane. It would then be possible to obtain a measure of the inherent take-off capabilities of a given airplane, exclusive of the troublesome factor of piloting procedure, by means of a rather simple method. The relation between ground-run distance and speed would be determined in one series of tests; other tests, made at some safe altitude providing steady-air conditions, would establish the relationship between angle of climb and speed. These quantities, which should be largely independent of piloting effects, could then be combined, with a suitable correction for a standard type of transition, to give the total distance required to take off over obstacles of any desired height.

The effects on the air-borne portion of the take-off of a wind increasing in velocity with height are: a reduction in the speed of the airplane relative to the ground, consequently a reduction in the horizontal distance covered in a given time; and an increased vertical velocity due to the velocity gradient. These effects in combination and the effect of the wind gradient alone are shown

in figure 13 for normal take-offs with the heaviest and the lightest loads. For the heavy-load condition, the over-all reduction in the distance required to clear a 50-foot obstacle is 25 percent; the reduction due to the wind gradient alone is 16 percent. For an obstacle height of 100 feet, the reductions are 21 percent and 11 percent, respectively. With the light load the distance to clear the 50-foot obstacle is reduced 19 percent by the over-all effect of wind and 9 percent by reason of the wind gradient alone. For a 100-foot obstacle the reductions are 21 percent and 10 percent, respectively.

Apparently the effects of even a very moderate wind are rather large and should be taken into account in the analysis of take-off data. The method used in this report, i.e., step-by-step integration, would be too laborious for general use in evaluating the corrections for wind, but it has been found that these corrections can be determined with sufficient accuracy through the aid of rather simple relations: Still regarding the effects of wind velocity and velocity gradient as separate, the correction to the air-borne distance for the effect of wind velocity is

$$\Delta D_1 = \int_0^T V_w dt$$

where  $V_w$  is the wind velocity at any time  $t$  and  $T$  is the time required, from the instant of leaving the ground, to attain the height  $H$ .

For the average wind gradient, previously defined, the correction becomes, for  $H = 50$  feet,

$$\Delta D_1 = 1.27 \times V_{w_0} T$$

where  $V_{w_0}$  is the wind velocity at the ground.

For  $H = 100$  feet

$$\Delta D_1 = 1.38 V_{w_0} T$$

The effect of a wind velocity gradient on the height attained in a given time  $T$  is found from the energy relations to be



$$\Delta H = \frac{V \cos \gamma \Delta V_w}{g}$$

where  $\Delta H$  is the difference between the heights attained with and without the benefit of a wind gradient, in the same period of time, which is very nearly equivalent to the same horizontal distance;  $V$  is the air speed at the height  $H$ ;  $\gamma$  is the flight-path angle relative to the air at the height  $H$ ;  $\Delta V_w$  is the difference between the wind speed at 5 feet from the ground and at the effective height  $H_e$ . The correction to the observed air-borne distance for the wind gradient is then

$$\Delta D_2 = \frac{\Delta H}{\tan \gamma_1}$$

where  $\gamma_1$  is the angle of climb that would obtain were there no wind gradient; it is given closely enough by

$$\gamma_1 = \gamma - \tan^{-1} \frac{dV_w}{dH} \times \frac{V \sin \gamma}{g}$$

For the average wind gradient

$$\Delta V_w = 0.41 V_{w_0}, \text{ at a height of 50 feet}$$

and  $\Delta V_w = 0.55 V_{w_0}, \text{ at a height of 100 feet.}$

The angle of climb for no wind is given, for an obstacle height of 50 feet, by

$$\gamma_1 = \gamma - \tan^{-1} 0.0037 V_{w_0} \times \frac{V \sin \gamma}{g}$$

and, for an obstacle height of 100 feet, by

$$\gamma_1 = \gamma - \tan^{-1} 0.0021 V_{w_0} \times \frac{V \sin \gamma}{g}$$

The over-all correction to no-wind conditions is then, for an obstacle height of 50 feet,

$$\Delta D = 1.27 V_{w_0} T + \frac{V \cos \gamma \times 0.41 V_{w_0}}{g \tan \left( \gamma - \tan^{-1} 0.0037 \frac{V_{w_0} V \sin \gamma}{g} \right)}$$

and, for an obstacle height of 100 feet,

$$\Delta D = 1.38 V_{w_0} T + \frac{V \cos \gamma \times 0.55 V_{w_0}}{g \tan \left( \gamma - \tan^{-1} 0.0021 \frac{V_{w_0} V \sin \gamma}{g} \right)}$$

The corrections as computed from the foregoing equations agreed closely with those determined by the step-by-step integrations, the difference being less than 2 percent of the air-borne distance in all the cases considered. In the absence of specific data on the variation of the wind velocity with altitude, it is believed that the assumption of an average wind gradient will provide a good approximation.

The effect of proximity of the ground on the distance required for the air-borne stages of the take-off is shown in figure 14. The ground effect reduces the distance required to attain an altitude of 50 feet by 10 percent with the lightest load and by 16 percent with the heaviest load. For an obstacle height of 100 feet, the percentage reductions are about one-half of those for the 50-foot obstacle. The greater difference for the heavier load is probably due to the fact that the airplane climbs more slowly than with the light load; hence it is in the region of strongest ground effect for a longer period.

#### CONCLUSIONS.

1. For normal take-offs the optimum conditions for the transition phase were realized at the slowest possible take-off speed. Likewise, the shortest over-all distance required in taking off over an obstacle was obtained with the slowest speed.

2. For normal ground conditions, zoom take-offs required shorter over-all distances than normal take-offs, particularly with heavy loads if the obstacle to be sur-

mounted was sufficiently high. With light loadings and low obstacle heights the zoom take-offs provided no advantage.

3. The error resulting from neglect of the transition in calculating the air-borne distance in take-off varied from 8 percent with the heaviest load considered to -8 percent with the lightest load for normal take-offs over a 50-foot obstacle. For a 100-foot obstacle the percentage error was about one-half of that for the 50-foot obstacle. For zoom take-offs the error arising from neglect of the transition was much greater.

4. The effect of the average wind gradient corresponding to a 5-mile-per-hour surface wind was a reduction in the air-borne distance to clear a 50-foot obstacle of about 9 percent with the lightest load and about 16 percent with the heaviest load. For the 100-foot obstacle height the reduction was about 10 percent for both loads. The over-all reduction due to this wind was approximately twice that due to the wind gradient alone. The correction of observed take-off performance to no-wind conditions can be accomplished through the use of relatively simple expressions.

5. The ground effect reduced the air-borne distance required to attain a height of 50 feet by about 10 percent with the lightest loading and by about 16 percent with the heaviest loading. For an obstacle height of 100 feet the percentage reduction was about one-half as great.

Langley Memorial Aeronautical Laboratory,  
National Advisory Committee for Aeronautics,  
Langley Field, Va., October 26, 1937.

## REFERENCES

1. Thompson, F. L., Peck, W. C., and Beard, A. P.: Air Conditions Close to the Ground and the Effect on Airplane Landings. T.R. No. 489, N.A.C.A., 1934.
2. Hartman, Edwin P.: Working Charts for the Determination of Propeller Thrust at Various Air Speeds. T.R. No. 481, N.A.C.A., 1934.
3. Freeman, Hugh B.: Comparison of Full-Scale Propellers Having R.A.F.-6 and Clark Y Airfoil Sections. T.R. No. 378, N.A.C.A., 1931.

## FIGURE LEGENDS

- Figure 1.- The Verville AT airplane.
- Figure 2.- Lift and drag characteristics of the Verville AT airplane as determined from take-off tests.
- Figure 3.- Excess-thrust characteristics of the Verville AT airplane.
- Figure 4.- Examples of assumed variation in lift coefficient during transition. The Verville AT airplane.
- Figure 5.- Weight, 2,060 pounds.
- Figure 6.- Weight, 2,378 pounds.
- Figure 7.- Weight, 2,800 pounds.
- Figures 5 to 7.- Flight paths followed in transition and steady climb for normal and zoom take-offs for the Verville AT airplane at various speeds.
- Figure 8.- Ground distance required for the Verville AT airplane to accelerate from 75 feet per second to take-off speed for all loading conditions.
- Figure 9.- Weight, 2,060 pounds.
- Figure 10.- Weight, 2,378 pounds.
- Figure 11.- Weight, 2,800 pounds.
- Figures 9 to 11.- Variation of take-off distances with take-off speed for the Verville AT airplane.
- Figure 12.- Error in air-borne distance due to neglect of transition for the Verville AT airplane.
- Figure 13.- Effect of wind and wind gradient on the flight path of the Verville AT airplane during transition and steady climb. Surface wind velocity, 5 miles per hour.
- Figure 14.- Effect of ground proximity on the flight path of the Verville AT airplane during transition and steady climb.

TABLE I - Characteristics of the Verville AT Airplane

Engine - Continental A-70 . . . . .	165 hp. at 2,000 r.p.m.
Propeller - Metal, fixed pitch:	
Blade section . . . . .	Clark Y
Diameter . . . . .	8 ft. 5 in.
Blade-angle setting at 0.75 R . . . . .	12.8°
Wing dimensions - Clark Y-15:	
Total area . . . . .	262.5 sq. ft.
Span, upper wing . . . . .	31 ft.
Span, lower wing . . . . .	31 ft.
Chord, upper wing . . . . .	50 in.
Chord, lower wing . . . . .	50 in.
Test loadings:	
Gross weight . . . . .	2,060 lb.
Wing loading . . . . .	7.8 lb. per sq. ft.
Power loading . . . . .	12.5 lb. per hp.
Gross weight . . . . .	2,378 lb.
Wing loading . . . . .	9.1 lb. per sq. ft.
Power loading . . . . .	14.4 lb. per hp.

TABLE II - Take-Off Distances for the Verville AT Airplane From Step-by-Step Integrations

Weight (lb.)	Power loading (lb./hp.)	Wing loading (lb./sq.ft.)	Take-off speed (air) (f.p.s.)	Climbing speed (air) (f.p.s.)	Ground-run distance from V = 75 f.p.s. (ft.)	Height attained in transition (ft.)	Horizontal distance for transition (ft.)	Tangent of angle of steady climb, $\gamma$	Obstacle height = 50 ft.			Obstacle height = 100 ft.			Remarks	
									Horizontal distance for steady climb (ft.)	Total air-borne distance (ft.)	Total distance from V = 75 f.p.s. (ft.)	Horizontal distance for steady climb (ft.)	Total air-borne distance (ft.)	Total distance from V = 75 f.p.s. (ft.)		
2,060	12.5	7.8	75.5	75.5	7	74.5	534	0.1441	---	370	377	176	710	717	Normal.	
			82.0	82.0	89	47.2	348	.1464	20	368	457	359	707	796		
			90.0	90.0	208	39.2	314	.1366	78	392	600	444	758	966		
			82.0	75.5	89	82.5	483	.1441	---	287	374	121	604	693		Zoom.
			90.0	75.5	208	101.0	490	.1441	---	237	445	---	482	690		
			2,378	14.4	9.1	81.0	81.0	98	46.2	491	.0930	40	531	629		572
88.0	88.0	217				36.5	396	.0969	139	535	752	654	1,050	1,267		
96.0	96.0	392				28.6	335	.0894	238	573	965	799	1,134	1,526		
88.0	81.0	217				65.0	519	.0930	---	367	584	376	895	1,112	Zoom.	
96.0	81.0	392				88.3	550	.0930	---	269	661	125	675	1,067		
2,800	17.0	10.7				88.0	88.0	274	28.0	526	.0455	482	1,008	1,282	1,581	2,107
			96.0	96.0	490	22.7	432	.0503	543	975	1,465	1,540	1,972	2,462		
			104.0	104.0	782	15.0	312	.0443	786	1,098	1,880	1,917	2,229	3,011		
			96.0	88.0	490	49.5	542	.0455	13	555	1,045	1,108	1,650	2,140	Zoom.	
			104.0	88.0	782	68.7	509	.0455	---	302	1,084	686	1,195	1,977		
			2,060	12.5	7.8	75.5	75.5	---	---	---	---	---	300	---	---	561
75.5	75.5	---				---	---	---	---	---	337	---	---	642	---	
2,800	17.0	10.7	88.0	88.0	---	---	---	---	---	756	---	---	1,665	---	5 m.p.h. wind + gradient. Wind gradient only.	
			88.0	88.0	---	---	---	---	---	---	844	---	---	1,878		---
2,060	12.5	7.8	75.5	75.5	---	63.3	495	---	---	404	---	254	749	---	No ground effect.	
2,800	17.0	10.7	88.0	88.0	---	10.6	308	---	---	865	1,173	---	1,962	2,270	No ground effect.	



Figure 1.- The Verville AT airplane.



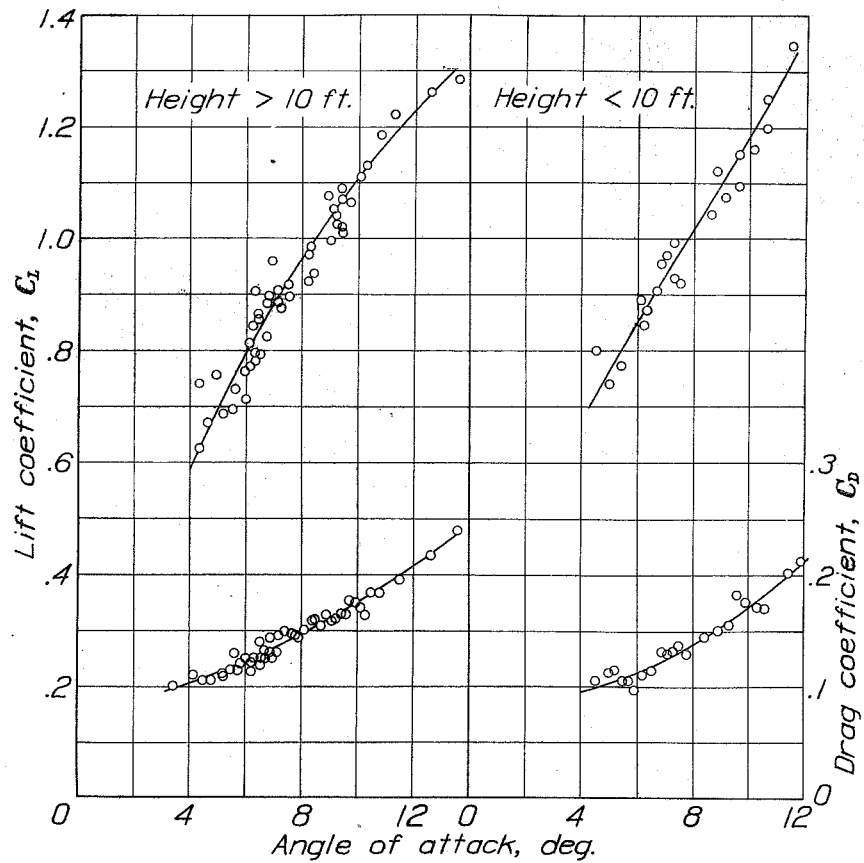


Figure 2.

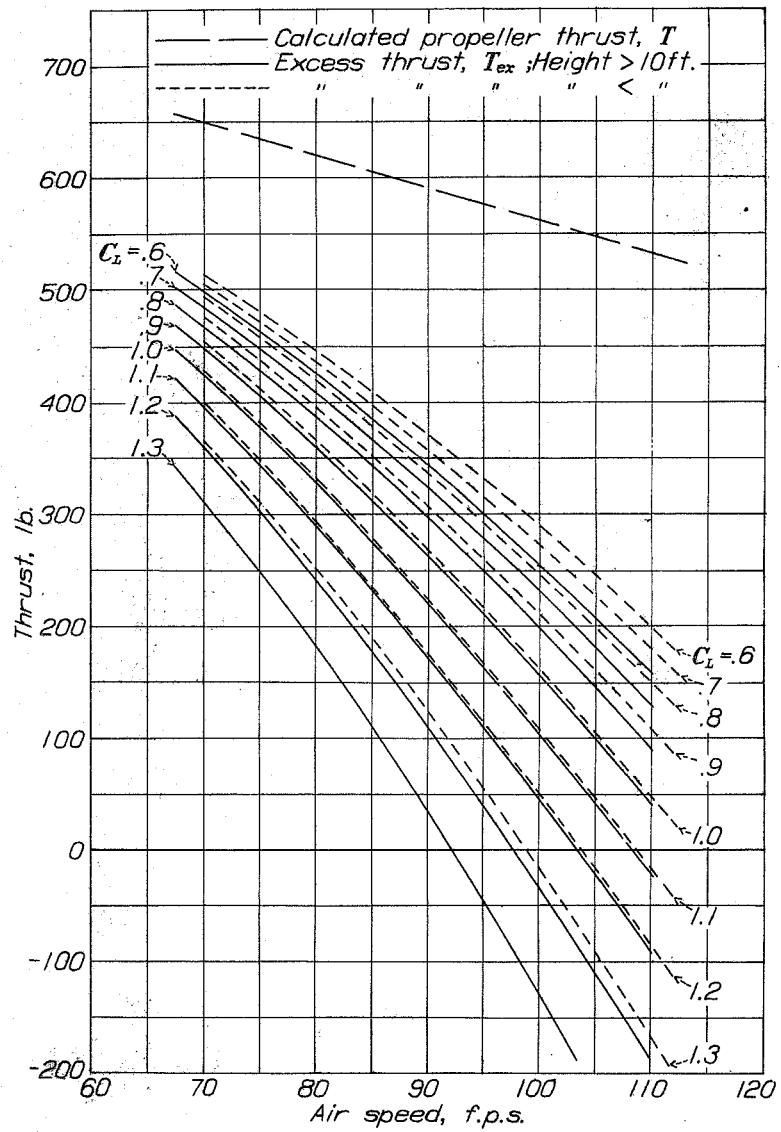


Figure 3.

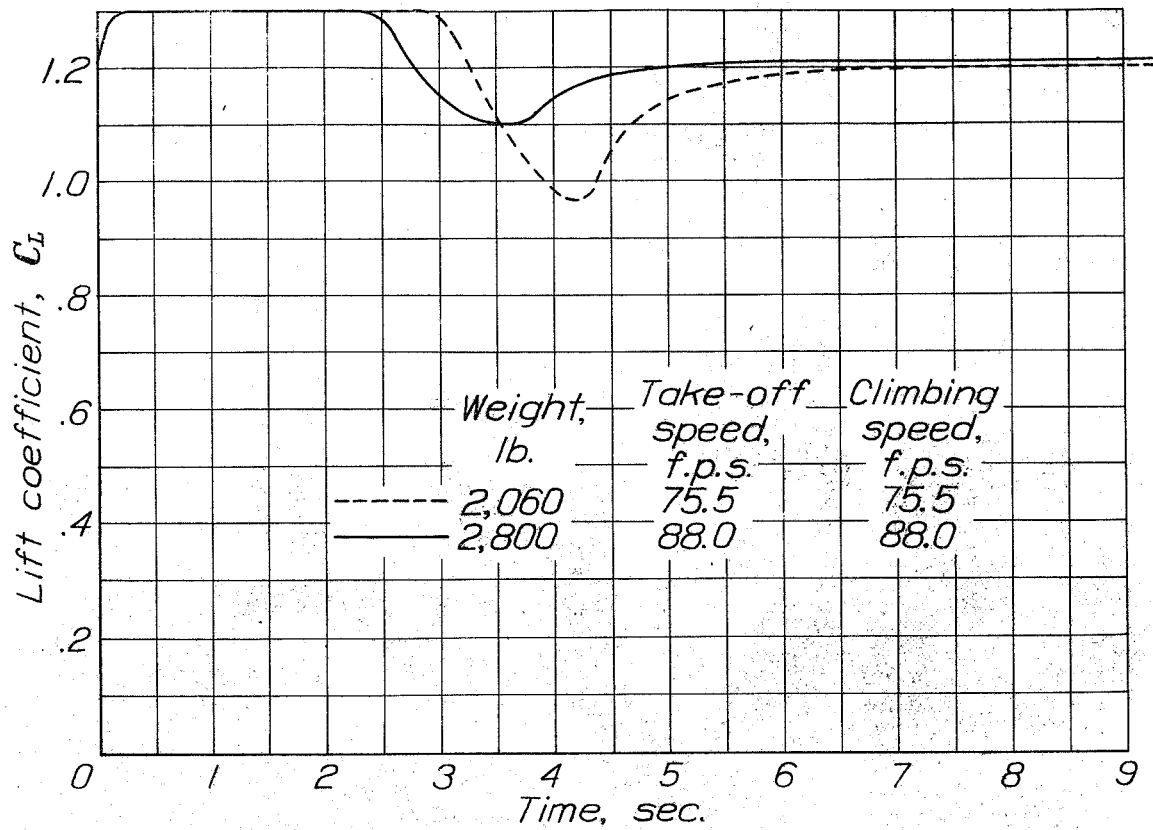


Figure 4.

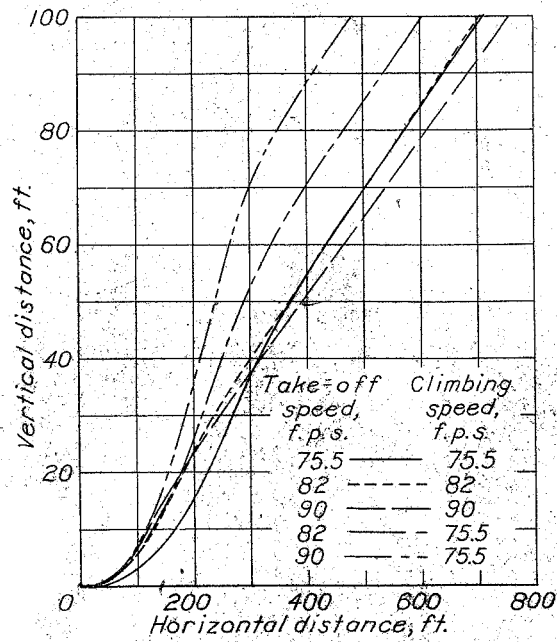


Figure 5.

*Calculated*  
5-7

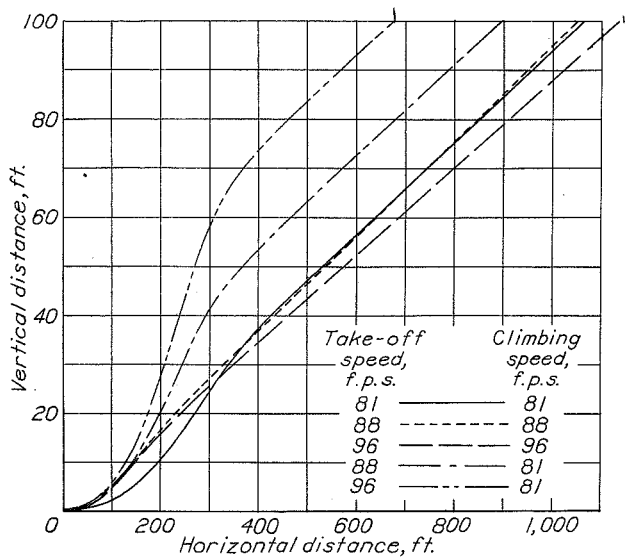


Figure 6.

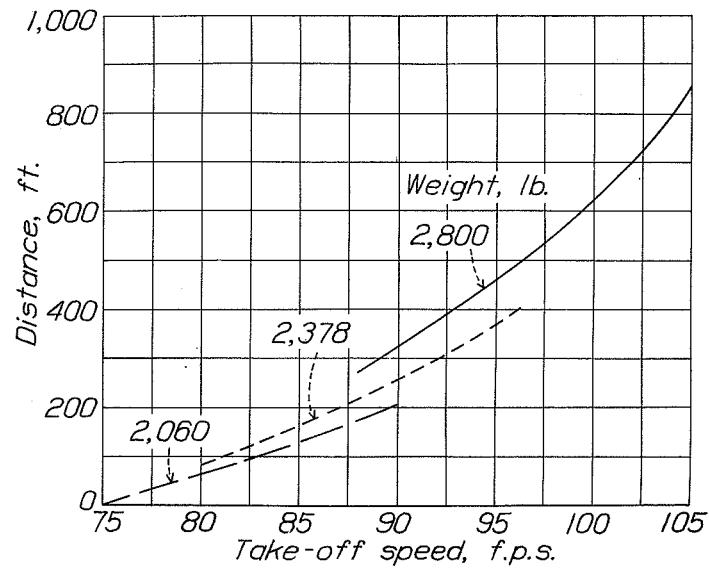


Figure 8.

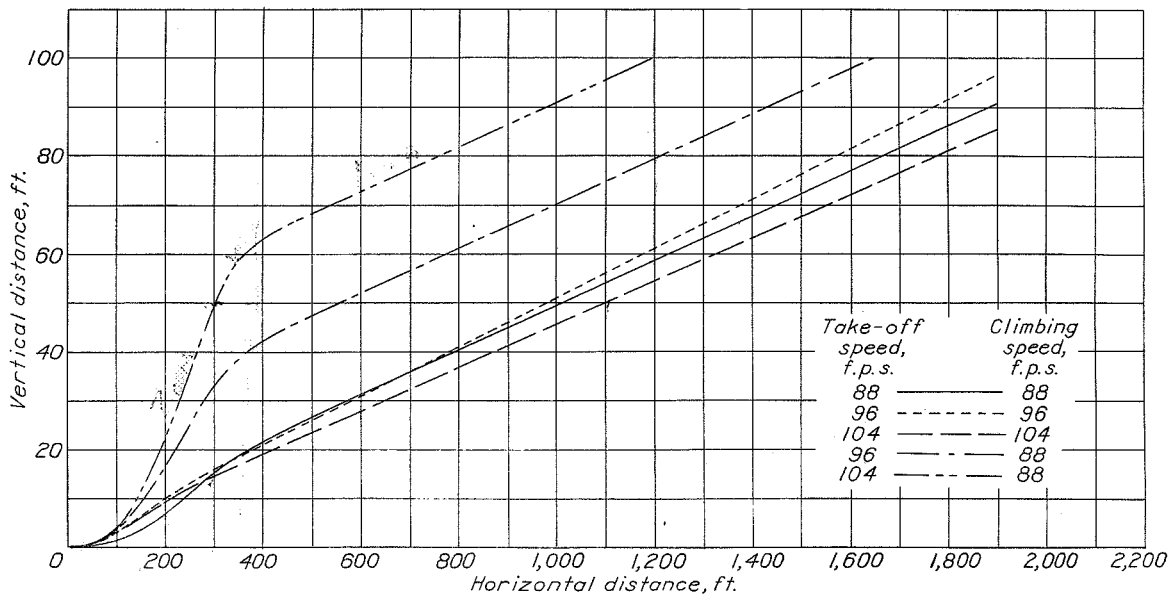


Figure 7.

est. 165 HP  
 est power load 14.9" HP  
 approx based on 1 wing (approx) = 66.5  
 2 \* 33.3 = 66.6

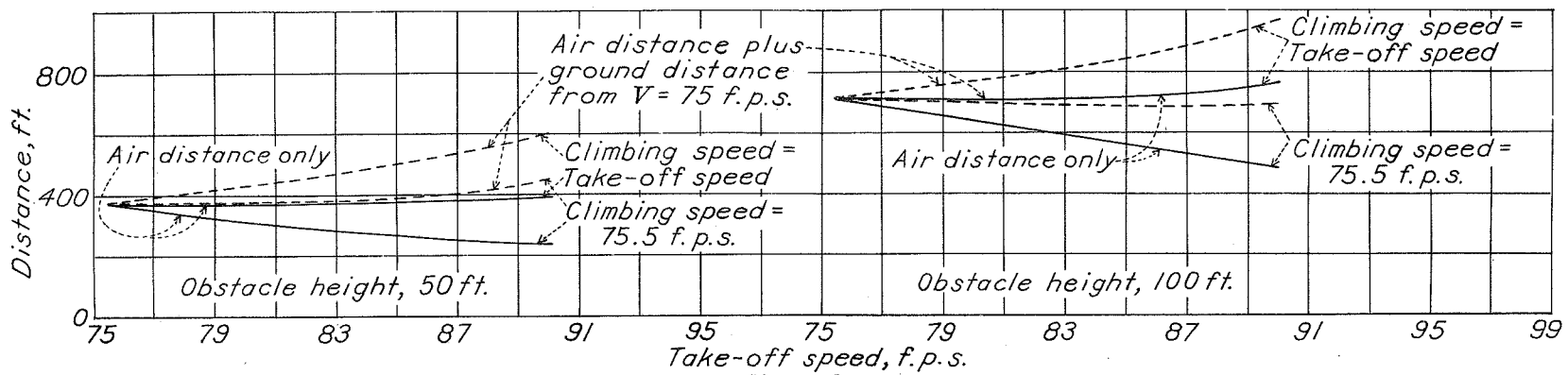


Figure 9.

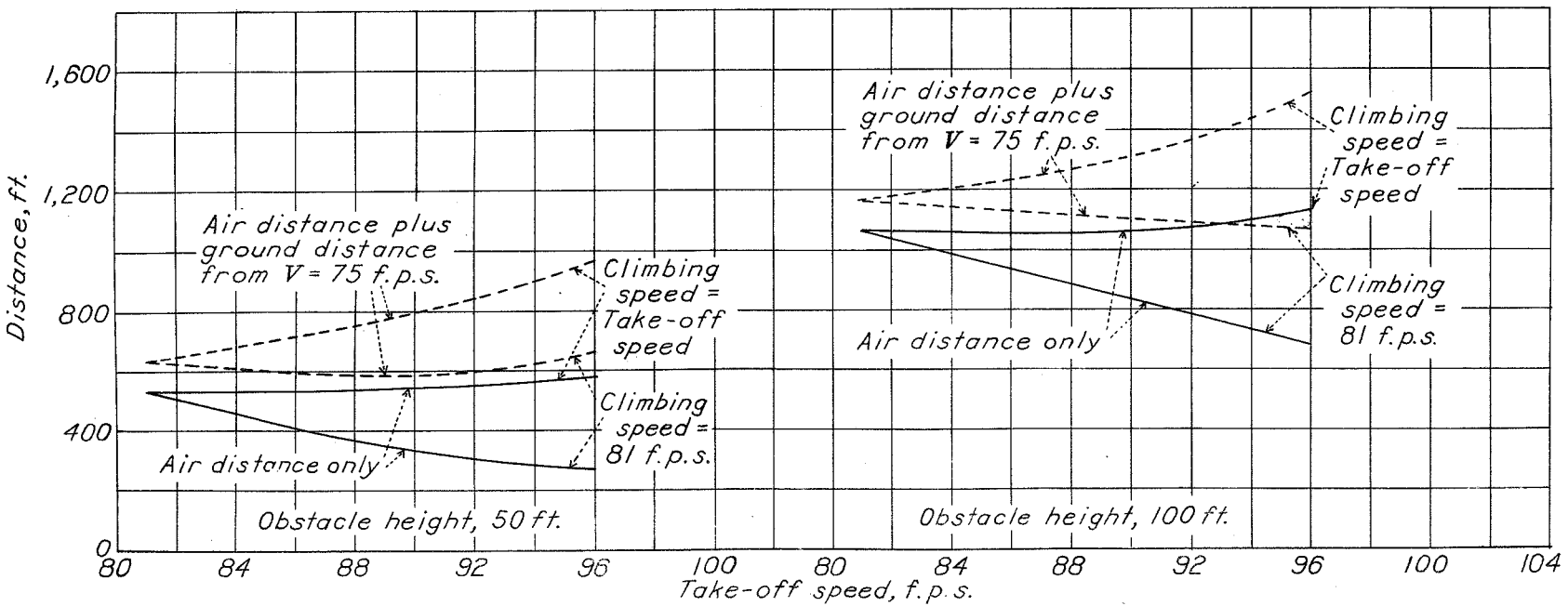


Figure 10.

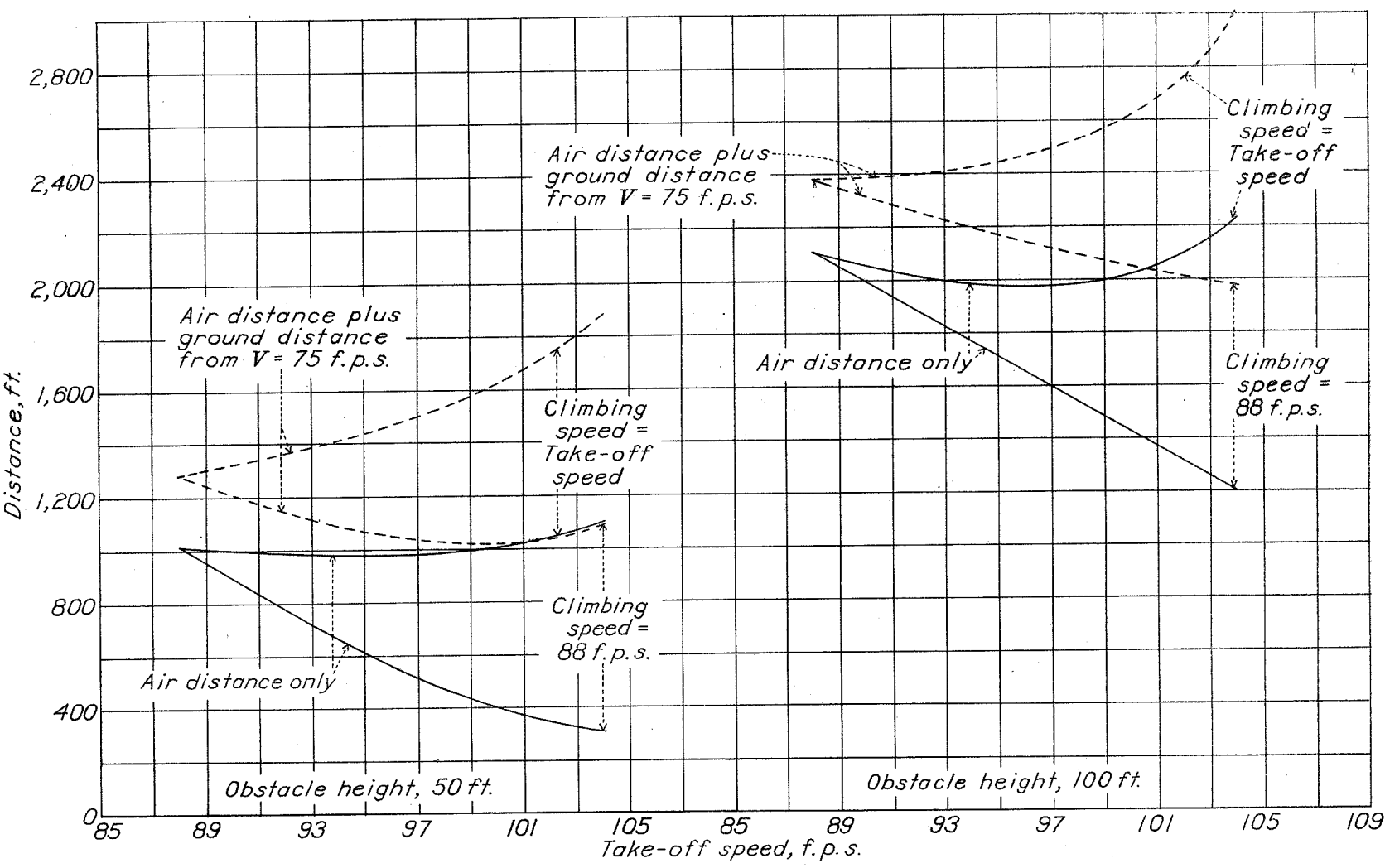


Figure 11.

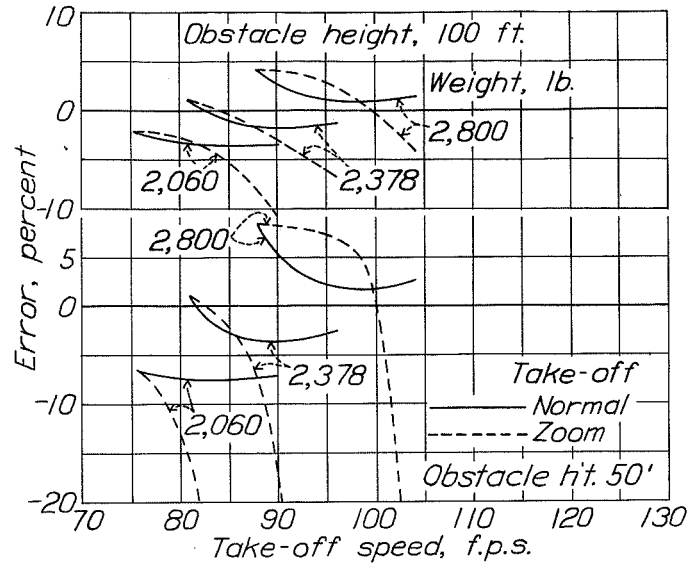


Figure 12.

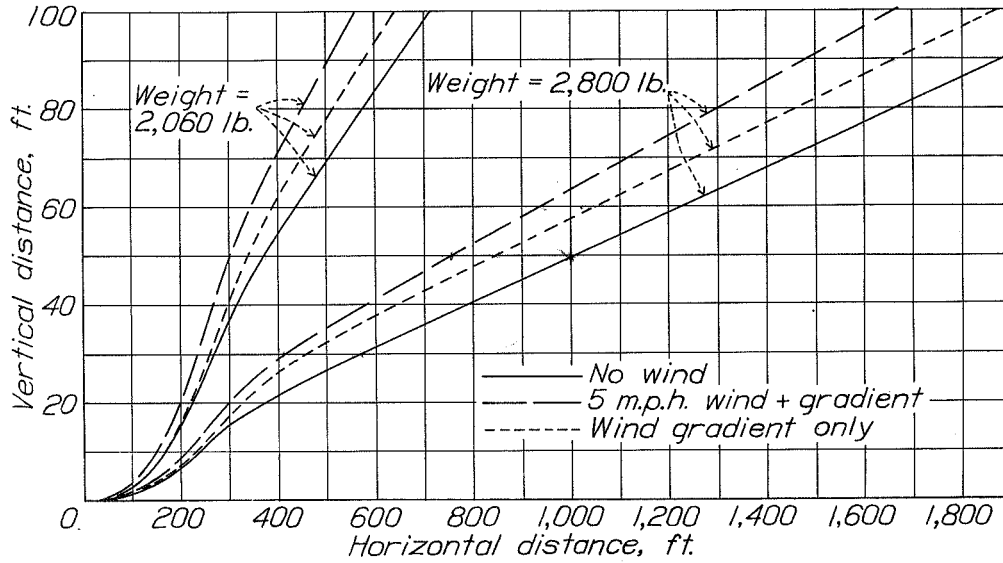


Figure 13.

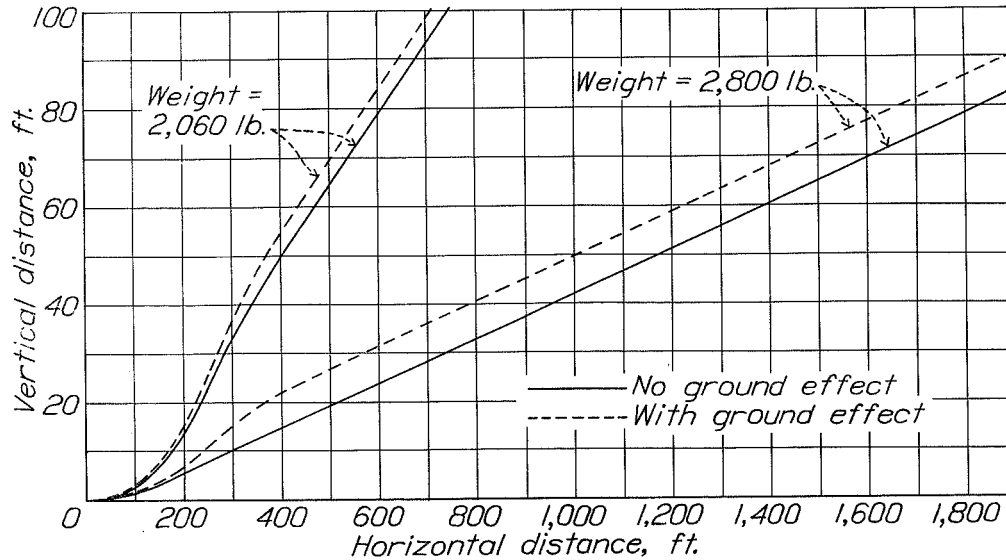


Figure 14.